Université Pierre et Marie Curie

Master Sciences et Technologie (M2)

Spécialité : Concepts fondamentaux de la physique

Parcours : Physique des Liquides et Matière Molle

Cours : Dynamique Non-Linéaire

Laurette TUCKERMAN

laurette@pmmh.espci.fr

VII. Reaction-Diffusion Equations:

English-language version

1. Excitability

2. Turing patterns

3. Lyapunov functionals

4. Spatial analysis and fronts

Reaction-Diffusion Systems

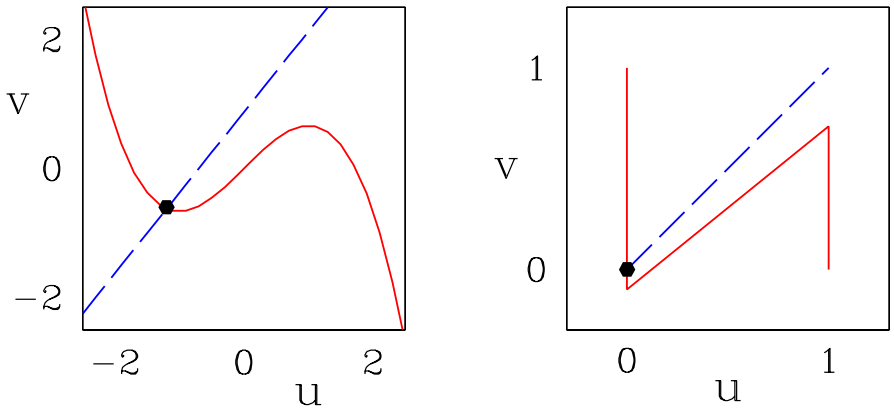

Figure 1: Nullclines of the FitzHugh-Nagumo (left) and Barkley (right) models. The solid curves are the u-nullclines $\partial_t u = f(u,v) = 0$ and the dashed curves are the v-nullclines $\partial_t v = g(u,v) = 0$. The intersections of the two types of nullclines are homogeneous steady states.

A reaction-diffusion system is a dynamical system of the form

$$\partial_t u_i = f_i(u_1, u_2, \ldots) + D_i \Delta u_i \tag{1}$$

The **reaction terms $\mathbf{f_i}$** couple the different **chemical species $\mathbf{u_i}$** at the same spatial location, and the Laplacian describes diffusion of u_i with species-specific diffusivity D_i. Reaction-diffusion equations describe oscillating chemical reactions, the most famous of which is the Belousov-Zhabotinskii reaction, discovered by two Soviet scientists in the late 1950s and early 1960s. Such systems are also used to describe phenomena in biology (population biology, epidemiology, neurosciences), social sciences (economics, demography) and physics.

Commonly studied models have two species:

$$\partial_t u = f(u,v) + D_u \Delta u \tag{2a}$$
$$\partial_t v = g(u,v) + D_v \Delta v \tag{2b}$$

For the moment, we consider the spatially homogeneous version of (2), where u, v are scalars.

$$\partial_t u = f(u,v) \tag{3a}$$
$$\partial_t v = g(u,v) \tag{3b}$$

Two such systems are the FitzHugh-Nagumo equations:

$$f(u,v) = u - u^3/3 - v + I \tag{4a}$$
$$g(u,v) = 0.08\,(u + 0.7 - 0.8\,v) \tag{4b}$$

and the Barkley model

$$f(u,v) = \frac{1}{\epsilon}\,u(1-u)\left(u - \frac{v+b}{a}\right) \tag{5a}$$
$$g(u,v) = u - v \tag{5b}$$

Steady states $(\bar{u}, \bar{v})$ are the intersections of the u-**nullcline** $f = 0$ and the v-**nullcline** $g = 0$, as shown in figure 1. These are stable if the eigenvalues of

$$\begin{pmatrix} f_u & f_v \\ g_u & g_v \end{pmatrix} \tag{6}$$

are both negative (or have negative real part).

1 Excitability

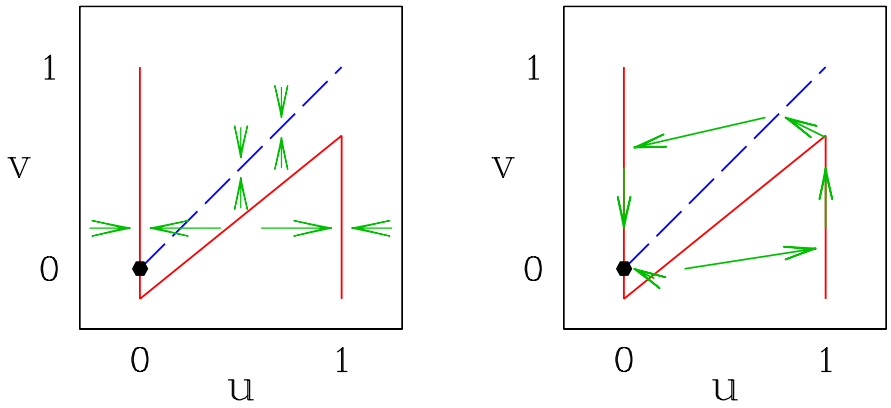

Figure 2: Dynamics of the Barkley model. Left: large horizontal arrows indicate where $\partial_t u = f$ is positive or negative. Small vertical arrows indicate where $\partial_t v = g$ is positive or negative. The u-nullcline has three portions: $u = 0$, $u = 1$, and the middle branch $u = (v + b)/a$, which is the excitation threshold. Right: Trajectory undergone after excitation. A sufficiently large perturbation from $u = v = 0$ causes u to cross the middle branch to the **excited phase** $u = 1$, during which v increases slowly to near 1. Then u crosses quickly back to the **refractory phase** at $u = 0$, during which v decreases slowly to near 0. When $(u, v) \approx (0, 0)$, the system is again **excitable**.

Figure 2 shows the nullclines of the Barkley model (5), along with arrows indicating the direction of motion in the (u, v) plane, i.e. rightwards (leftwards) arrows where $\partial_t u = f > (<)\, 0$ and upwards (downwards) arrows where $\partial_t v = g > (<) 0$. Because of the factor $1/\epsilon$ in the u-equation (5a), horizontal (u) motion takes place on a fast timescale compared to vertical (v) motion, as symbolized by the long and short arrows. The portions of the (u, v) plane for which vertical (v) motion is important are those where u motion is zero or negligeable, i.e. on or near the u-nullcline. The u-nullcline is made up of three branches:$u = 0$, $u = 1$ and $u = (v + b)/a$, which is the **excitation threshold**. Figure 2 shows that the **middle branch** $u = (v + b)/a$ of the u-nullcline acts as a threshold. If the steady state $(\bar{u}, \bar{v}) = (0, 0)$ is slightly perturbed, then the resulting trajectory will converge directly back to the steady state. If, however, the perturbation is large enough that the middle branch is traversed, then the resulting trajectory will undergo a long excursion, first quickly rightwards, then slowly upwards along the $u = 1$ nullcline, then quickly leftwards, then slowly downwards along the $u = 0$ nullcline, finally returning to $(0, 0)$. The dynamics consist of three phases. When (u, v) is near zero, the system is said to be **excitable**: a sufficiently large perturbation will lead to an excursion. When $u \approx 1$, the system is said to be **excited**.

When $u \approx 0$, but $v \not\approx 0$, the system is said to be **refractory**: the middle branch, i.e. the threshold, is too far for the system to be excited.

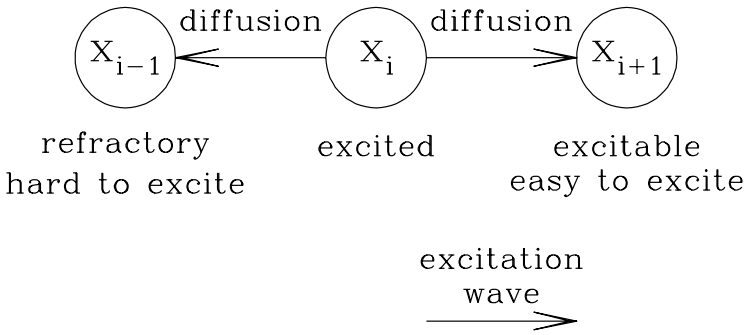

Figure 3: Waves in an excitable medium. Although diffusion from x_i acts in both directions, if x_{i-1} has recently been excited, then it is refractory and hard to excite. Only x_{i+1} will be excited and the wave will continue to propagate to the right.

How might the system become excited? With the inclusion of spatial variation and diffusion, excitability leads to propagating waves. If one location (a numerical or biological cell x_i) is excited, then diffusion will cause it to excite its neighbors. If the neighbor on one side (say x_{i-1}) has recently been excited, then it is in the refractory phase and cannot become excited. Instead, only the neighbor on the other side (x_{i+1}), where the wave has not yet passed (recently), will become excited. Meanwhile, cell x_i enters the refractory phase and cell x_{i+1} excites cell x_{i+2}. Thus, the wave propagates in one direction.

Excitability plays an important role in physiology. In particular, cardiac tissue (the heart) is excitable, as are neurons. A part of the heart serves as the **pacemaker**, periodically emitting electrical signals, and these are propagated to the rest of the heart.

2 Turing patterns

We now consider spatially inhomogeneous solutions to reaction-diffusion systems. A steady state $\bar{U} = (\bar{u}, \bar{v})$ of (3) is also a steady (homogeneous) state of (2), since the Laplacian of a constant is zero. What about stability? If $(\bar{u}, \bar{v})$ is a stable solution of (3), is it also a stable solution of (2), i.e. is it stable to spatially dependent perturbations when diffusion is included? In general, diffusion has the effect of smoothing out variations, so we would expect that the homogeneous steady state would remain stable. We now carry out a linear stability analysis by substituting $u(x,t) = \bar{u} + \tilde{u}e^{\sigma t + i\mathbf{k}\cdot\mathbf{x}}$, $v(x,t) = \bar{v} + \tilde{v}e^{\sigma t + i\mathbf{k}\cdot\mathbf{x}}$ into (2) and linearizing:

$$\sigma\tilde{u} = f_u\tilde{u} + f_v\tilde{v} - D_u k^2\tilde{u} \quad (7a)$$

$$\sigma\tilde{v} = g_u\tilde{u} + g_v\tilde{v} - D_v k^2\tilde{v} \quad (7b)$$

where f_u, f_v, g_u, g_v are the partial derivatives of f and g evaluated at the steady state $(\bar{u}, \bar{v})$, which may have either sign. That is, we seek the eigenvalues $\sigma_{k\pm}$ of the matrix

$$M_k \equiv \begin{pmatrix} f_u - D_u k^2 & f_v \\ g_u & g_v - D_v k^2 \end{pmatrix} = \begin{pmatrix} f_u & f_v \\ g_u & g_v \end{pmatrix} - k^2 \begin{pmatrix} D_u & 0 \\ 0 & D_v \end{pmatrix} \quad (8)$$

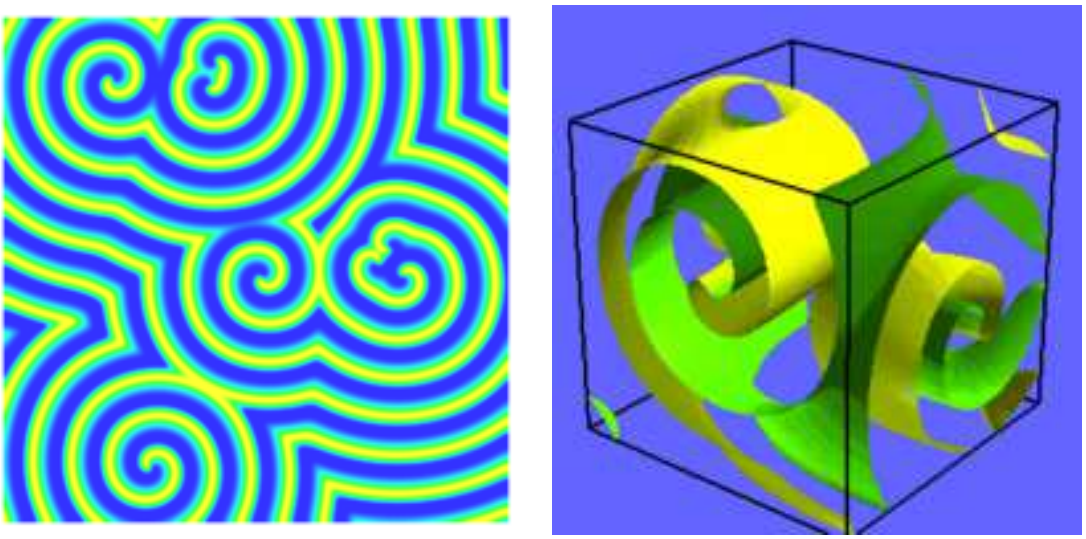

Figure 4: Simulations from Barkley model. Left: Domain with competing spiral waves in 2D. Right: scroll waves in 3D. From D. Barkley, *Barkley model*, Scholarpedia.

If $D_u = D_v \equiv D$ then M_k differs from M_0 by $(-D\ k^2)$ times the identity. Then M_k has the same eigenvectors as M_0, with the eigenvalues shifted by $(-D\ k^2)$. Since $(\bar{u}, \bar{v})$ is stable to homogeneous perturbations, the eigenvalues of M_0 are negative The eigenvalues of M_k are then also negative and $(\bar{u}, \bar{v})$ is stable to inhomogeneous perturbations. This can also be seen from the explicit expression for the eigenvalues of $M_k = \begin{pmatrix} a & b \\ c & d \end{pmatrix}$:

$$\begin{aligned} \sigma_{k\pm} &= \frac{a+d}{2} \pm \sqrt{\left(\frac{a-d}{2}\right)^2 + bc} \\ &= \frac{f_u + g_v}{2} - k^2 \frac{D_u + D_v}{2} \pm \sqrt{\left(\frac{f_u - g_v - (D_u - D_v)k^2}{2}\right)^2 + f_u g_v} \end{aligned} \tag{9}$$

which shows that $\sigma_{k\pm} = \sigma_0 - D\ k^2$ if $D_u = D_v = D$. This confirms the intuition that diffusion is a stabilizing influence. However, Alan Turing (a famous World War II British cryptologist considered by some to be the founder of computer science) realized in 1952 that the homogeneous state could be unstable if $D_u \neq D_v$, leading to what is now called a **Turing pattern**. We now seek the conditions under which this can occur.

We recall that a two-by-two matrix has one or more positive eigenvalues (or eigenvalues with positive real part) if Tr_k, the sum of the eigenvalues, satisfies $\mathrm{Tr}_k > 0$ or if Det_k, their product, satisfies $\mathrm{Det}_k < 0$; see figure 5. Since $\bar{U}$ is stable to homogeneous perturbations, we already know that

$$\mathrm{Tr}_0 = f_u + g_v < 0 \tag{10}$$

and that

$$\mathrm{Det}_0 = f_u g_v - f_v g_u > 0. \tag{11}$$

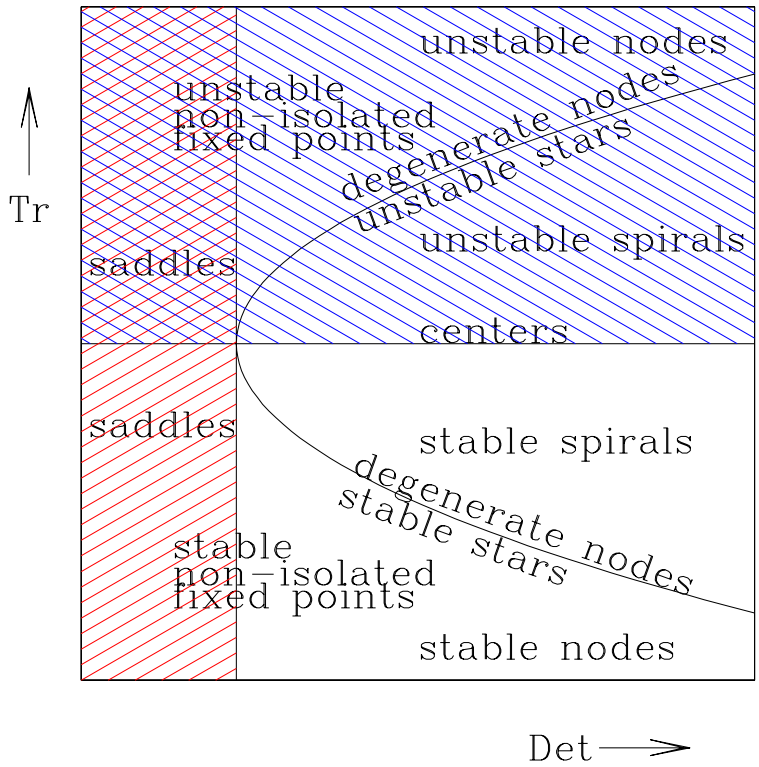

Figure 5: Behavior of two-dimensional linear systems as a function of the trace Tr and the determinant Det of the matrix. For $Det < 0$, the two eigenvalues are real and of opposite sign, leading to a saddle. For $Det > Tr^2/4$, the eigenvalues are complex conjugates and the behavior is thus oscillatory. For $Tr > 0$ at least one of the eigenvalues has a positive real part and the fixed point is thus unstable. Limiting cases are non-isolated fixed points ($Det = 0$), stars and degenerate nodes ($Tr^2 = 4Det$), and centers ($Tr = 0$, $Det > 0$).

We have

$$\mathrm{Tr}_k = f_u + g_v - (D_u + D_v)k^2 = \mathrm{Tr}_0 - (D_u + D_v)k^2 < \mathrm{Tr}_0 < 0 \tag{12}$$

so in order for $\bar{U}$ to be unstable to inhomogeneous perturbations, we must have $\mathrm{Det}_k < 0$ for some values of k.

$$\begin{aligned} \mathrm{Det}_k &= f_u g_v - f_v g_u - (D_v f_u + D_u g_v)k^2 + D_u D_v k^4 \\ &= \mathrm{Det}_0 + D_u D_v k^4 - (D_v f_u + D_u g_v)k^2 \end{aligned} \tag{13}$$

We know that $\mathrm{Det}_0 > 0$ and that $\mathrm{Det}_k > 0$ for large k, so we seek an intermediate range of k for which $\mathrm{Det}_k < 0$. The minimum of Det_k is obtained by differentiating (13) with respect to k^2:

$$\begin{aligned} 0 &= 2D_u D_v k^2 - (D_v f_u + D_u g_v) \\ k^2 &= \frac{D_v f_u + D_u g_v}{2D_u D_v} \end{aligned} \tag{14}$$

We require that this value of k^2 be positive

$$D_v f_u + D_u g_v > 0 \tag{15}$$

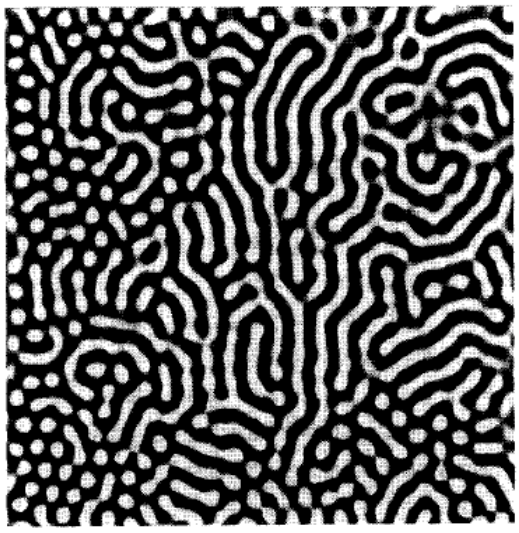

Figure 6: Turing pattern in a chlorite-iodide-malonic acid chemical laboratory experiment. From R.D. Vigil, Q. Ouyang & H.L. Swinney, *Turing patterns in a simple gel reactor*, Physica A **188**, 17 (1992).

and that Det_k be negative at this value:

$$\begin{aligned}
0 &> \mathrm{Det}_0 + D_u D_v \left(\frac{D_v f_u + D_u g_v}{2 D_u D_v} \right)^2 - (D_v f_u + D_u g_v) \frac{D_v f_u + D_u g_v}{2 D_u D_v} \\
&= \mathrm{Det}_0 + \frac{(D_v f_u + D_u g_v)^2}{4 D_u D_v} - \frac{(D_v f_u + D_u g_v)^2}{2 D_u D_v} \\
&= \mathrm{Det}_0 - \frac{(D_v f_u + D_u g_v)^2}{4 D_u D_v} \\
0 &> 4 D_u D_v (f_u g_v - f_v g_u) - (D_v f_u + D_u g_v)^2 \\
(D_v f_u + D_u g_v)^2 &> 4 D_u D_v (f_u g_v - f_v g_u) \qquad (16)
\end{aligned}$$

Thus, (10), (11), (15), and (16) are the conditions for a Turing pattern.

Note that if $D_u = D_v$, then condition (15) cannot be satisfied since $f_u + g_v = \mathrm{Tr}_0 < 0$. The wavenumbers of the patterns are given by (14).

Turing patterns were first produced in experiments in 1990 by de Kepper et al. at the University of Bordeaux and shortly thereafter by Swinney et al. at the University of Texas at Austin, see figure 6. This mechanism is thought to be responsible for differentiation within embryos and the formation of patterns on animal coats (such as zebras and leopards).

3 Lyapunov functionals

The behavior of one-dimensional dynamical systems is necessarily simple. There can be no limit cycles, and generally the behavior consists merely of converging to a fixed point. A class of multidimensional

systems, called **variational, potential**, or **gradient** flows:

$$\frac{d\mathbf{u}}{dt} = -\nabla\Phi \qquad \Longleftrightarrow \qquad \frac{du_i}{dt} = -\frac{\partial\Phi}{\partial u_i} \tag{17}$$

can also be shown to behave in this way.

The Jacobian of (17) is the **Hessian** matrix

$$-\begin{pmatrix} \partial^2\Phi/(\partial u_1\partial u_1) & \partial^2\Phi/(\partial u_1\partial u_2) & \dots \\ \partial^2\Phi/(\partial u_2\partial u_1) & \partial^2\Phi/(\partial u_2\partial u_2) & \dots \\ \vdots & \vdots & \vdots \end{pmatrix} \tag{18}$$

As a symmetric matrix, the Hessian cannot have complex eigenvalues and hence the gradient system (17) cannot undergo a Hopf bifurcation. A more general argument forbidding limit cycles is as follows:

$$\frac{d\Phi}{dt} = \sum_i \frac{\partial\Phi}{\partial u_i}\frac{du_i}{dt} = -\sum_i \frac{\partial\Phi}{\partial u_i}\frac{\partial\Phi}{\partial u_i} = -|\nabla\Phi|^2 \tag{19}$$

so that Φ decreases monotonically. Limit cycles cannot occur since Φ decreases, either to $-\infty$ or to a point where $\nabla\Phi = 0$, at which $d\mathbf{u}/dt = 0$.

We can generalize (17) to spatially dependent systems, in particular to reaction-diffusion systems whose reaction term is a gradient of a potential $\Phi(u)$:

$$\frac{\partial\mathbf{u}}{\partial t} = -\nabla\Phi + \frac{\partial^2\mathbf{u}}{\partial x^2} \tag{20}$$

The domain of (20) is the (possibly infinite) interval $(x_{\rm lo}, x_{\rm hi})$ and either Dirichlet boundary conditions

$$\mathbf{u}(x_{\rm lo}) = \mathbf{u}_{\rm lo} \qquad \mathbf{u}(x_{\rm hi}) = \mathbf{u}_{\rm hi} \tag{21}$$

or homogeneous Neumann boundary conditions

$$\frac{\partial\mathbf{u}}{\partial x}(x_{\rm lo}) = 0 \qquad \frac{\partial\mathbf{u}}{\partial x}(x_{\rm hi}) = 0 \tag{22}$$

are imposed.

To take the place of Φ, we define the **free energy** or **Lyapunov functional**,

$$\mathcal{F}(\mathbf{u}) \equiv \int_{x_{\rm lo}}^{x_{\rm hi}} dx \left[\Phi(\mathbf{u}(x,t)) + \frac{1}{2}\left|\frac{\partial\mathbf{u}(x,t))}{\partial x}\right|^2\right] \tag{23}$$

The two terms in the integral in (23) can be thought of as a potential energy and a kinetic energy. (This will be discussed further below.) In order to show that (20) is variational, we expand:

$$\begin{aligned} \mathcal{F}(\mathbf{u}+\delta\mathbf{u}) &= \int_{x_{\rm lo}}^{x_{\rm hi}} dx \left[\Phi(\mathbf{u}+\delta\mathbf{u}) + \frac{1}{2}\left|\frac{\partial(\mathbf{u}+\delta\mathbf{u})}{\partial x}\right|^2\right] \\ &= \int_{x_{\rm lo}}^{x_{\rm hi}} dx \left[\Phi(\mathbf{u}) + \nabla\Phi(\mathbf{u})\cdot\delta\mathbf{u} + \ldots + \frac{1}{2}\left|\frac{\partial\mathbf{u}}{\partial x} + \frac{\partial\delta\mathbf{u}}{\partial x} + \ldots\right|^2\right] \\ &= \int_{x_{\rm lo}}^{x_{\rm hi}} dx \left[\Phi(\mathbf{u}) + \frac{1}{2}\left|\frac{\partial\mathbf{u}}{\partial x}\right|^2\right] + \int_{x_{\rm lo}}^{x_{\rm hi}} dx \left[\nabla\Phi(\mathbf{u})\cdot\delta\mathbf{u} + \frac{\partial\mathbf{u}}{\partial x}\cdot\frac{\partial\delta\mathbf{u}}{\partial x}\right] + O(\delta\mathbf{u})^2 \end{aligned} \tag{24}$$

We integrate by parts:

$$\int_{x_{\rm lo}}^{x_{\rm hi}} dx\, \frac{\partial \mathbf{u}}{\partial x} \cdot \frac{\partial \delta\mathbf{u}}{\partial x} = \left[\frac{\partial \mathbf{u}}{\partial x} \cdot \delta\mathbf{u}\right]_{x_{\rm lo}}^{x_{\rm hi}} - \int_{x_{\rm lo}}^{x_{\rm hi}} dx \frac{\partial^2 \mathbf{u}}{\partial x^2} \cdot \delta\mathbf{u} \tag{25}$$

The surface term in (25) obviously vanishes when homogeneous Neumann boundary conditions are imposed on $\mathbf{u}$. It also vanishes when Dirichlet boundary conditions are imposed on $\mathbf{u}$, since then homogeneous Dirichlet boundary conditions are imposed on the perturbation $\delta\mathbf{u}$.

We obtain:

$$\mathcal{F}(\mathbf{u}+\delta\mathbf{u}) = \int_{x_{\rm lo}}^{x_{\rm hi}} dx\, \left[\Phi(\mathbf{u}) + \left|\frac{\partial \mathbf{u}}{\partial x}\right|^2\right] + \int_{x_{\rm lo}}^{x_{\rm hi}} dx\, \left[\nabla\Phi(\mathbf{u}) - \frac{\partial^2 \mathbf{u}}{\partial x^2}\right] \cdot \delta\mathbf{u} + O(\delta\mathbf{u})^2 \tag{26}$$

The functional derivative $\delta\mathcal{F}/\delta\mathbf{u}$ is defined to be such that

$$\mathcal{F}(\mathbf{u}+\delta\mathbf{u}) = \mathcal{F}(\mathbf{u}) + \int_{x_{\rm lo}}^{x_{\rm hi}} dx\, \frac{\delta\mathcal{F}}{\delta\mathbf{u}} \cdot \delta\mathbf{u} + O(\delta\mathbf{u})^2 \tag{27}$$

for every perturbation $\delta\mathbf{u}$. Comparing (27) with (26), we obtain:

$$\int_{x_{\rm lo}}^{x_{\rm hi}} dx\, \frac{\delta\mathcal{F}}{\delta\mathbf{u}} \cdot \delta\mathbf{u} = \int_{x_{\rm lo}}^{x_{\rm hi}} dx\, \left[\nabla\Phi(\mathbf{u}) - \frac{\partial^2 \mathbf{u}}{\partial x^2}\right] \cdot \delta\mathbf{u} \tag{28}$$

Since the integrals in (28) are equal for every perturbation $\delta\mathbf{u}$, including a delta function centered on any point x and pointing in any of the vector directions, we must have the pointwise equality:

$$\frac{\delta\mathcal{F}}{\delta\mathbf{u}} = \nabla\Phi(\mathbf{u}) - \frac{\partial^2 \mathbf{u}}{\partial x^2} \tag{29}$$

which, using (20), implies

$$\frac{\delta\mathcal{F}}{\delta\mathbf{u}} = -\frac{\partial \mathbf{u}}{\partial t} \tag{30}$$

$\mathcal{F}$ evolves in time as follows:

$$\begin{aligned}
\frac{d\mathcal{F}}{dt} &= \lim_{\Delta t\to 0} \frac{1}{\Delta t}\left[\mathcal{F}(t+\delta t) - \mathcal{F}(t)\right] = \lim_{\Delta t\to 0} \frac{1}{\Delta t}\left[\mathcal{F}(\mathbf{u}(t+\Delta t)) - \mathcal{F}(\mathbf{u}(t))\right] \\
&= \lim_{\Delta t\to 0} \frac{1}{\Delta t}\left[\mathcal{F}\left(\mathbf{u}(t) + \frac{\partial \mathbf{u}}{\partial t}\Delta t + \ldots\right) - \mathcal{F}(\mathbf{u}(t))\right] \\
&= \lim_{\Delta t\to 0} \frac{1}{\Delta t}\left[\mathcal{F}(\mathbf{u}(t)) + \int_{x_{\rm lo}}^{x_{\rm hi}} dx \frac{\delta\mathcal{F}}{\delta\mathbf{u}} \cdot \frac{\partial \mathbf{u}}{\partial t}\Delta t + \ldots - \mathcal{F}(\mathbf{u}(t))\right] \\
&= \lim_{\Delta t\to 0} \frac{1}{\Delta t}\left[\int_{x_{\rm lo}}^{x_{\rm hi}} dx \frac{\delta\mathcal{F}}{\delta\mathbf{u}} \cdot \frac{\partial \mathbf{u}}{\partial t}\Delta t + \ldots\right] \\
&= \int_{x_{\rm lo}}^{x_{\rm hi}} dx \frac{\delta\mathcal{F}}{\delta\mathbf{u}} \cdot \frac{\partial \mathbf{u}}{\partial t} = \int_{x_{\rm lo}}^{x_{\rm hi}} dx \left(-\frac{\partial \mathbf{u}}{\partial t}\right) \cdot \frac{\partial \mathbf{u}}{\partial t} = -\int_{x_{\rm lo}}^{x_{\rm hi}} dx \left|\frac{\partial \mathbf{u}}{\partial t}\right|^2 \leq 0
\end{aligned} \tag{31}$$

where we have used (27) and (30). Just as we argued previously, limit cycles cannot occur since $\mathcal{F}$ decreases, either to $-\infty$ or to one of its local minima, where $\partial\mathbf{u}/\partial t = 0$. Although we used one spatial dimension for simplicity, the reasoning above can be applied in higher dimensions, by using volume integration and Gauss's Divergence Theorem to generalize (25).

4 Spatial Analysis and Fronts

We now return to equation

$$\frac{\partial u}{\partial t} = -\frac{d\Phi}{du} + \frac{\partial^2 u}{\partial x^2} \tag{32}$$

We consider u to be a scalar, although generalizations are possible to a vector $\mathbf{u}$. However, our treatment is necessarily restricted to the single spatial coordinate x, since the subject of this subsection is to draw an analogy between space and time.

We consider travelling wave solutions:

$$u(x,t) = U(x - ct) \tag{33}$$

which include steady states, for which $c = 0$. Defining

$$\xi \equiv x - ct \tag{34}$$

we have

$$\frac{\partial u}{\partial t}(x,t) = -c\,\frac{dU}{d\xi}(\xi) \tag{35a}$$

$$\frac{\partial^2 u}{\partial x^2}(x,t) = \frac{d^2U}{d\xi^2}(\xi) \tag{35b}$$

The equation obeyed by steady states and travelling waves becomes

$$\frac{d^2u}{d\xi^2} = \frac{d\Phi}{du} - c\,\frac{du}{d\xi} \tag{36}$$

where we have reverted from U to u and where $c = 0$ for a steady state.

We now carry out the fundamental, but merely notational, transformation used in **spatial analysis**, also called the **mechanical analogy**: we consider u to be like a position and ξ to be like a time. The mechanical interpretation of (36) is clear: the derivatives $du/d\xi$ and $d^2u/d\xi^2$ are like the velocity and the acceleration, respectively. The potential energy is $-\Phi$, rather than Φ, because of the sign convention used for Φ in the original reaction-diffusion system. The term $-c\,du/d\xi$ is like a frictional damping force, which is proportional to velocity. We can define something like an energy, which obeys:

$$\begin{aligned}
\frac{dE}{d\xi} &= \frac{d}{d\xi}\left[-\Phi + \frac{1}{2}\left(\frac{du}{d\xi}\right)^2\right] \\
&= -\frac{d\Phi}{du}\frac{du}{d\xi} + \frac{du}{d\xi}\frac{d^2u}{d\xi^2} \\
&= \left[-\frac{d\Phi}{du} + \frac{d^2u}{d\xi^2}\right]\frac{du}{d\xi} = -c\left(\frac{du}{d\xi}\right)^2
\end{aligned} \tag{37}$$

so it is conserved if $c = 0$, decreases if $c > 0$ and increases if $c < 0$. The fact that E can increase underlines the fact that the identification of u, ξ, and E with position, time, and energy is only an analogy. In terms of the original problem, $c < 0$ implies only motion towards the left.

It is possible to integrate (36) analytically for the case $c = 0$, when E is a constant. Starting from (37), we have

$$\begin{aligned} E &= -\Phi(u(\xi)) + \frac{1}{2}\left(\frac{du}{d\xi}\right)^2 \\ E + \Phi(u(\xi)) &= \frac{1}{2}\left(\frac{du}{d\xi}\right)^2 \\ \sqrt{2(E + \Phi(u(\xi)))} &= \frac{du}{d\xi} \\ \int d\xi &= \int \frac{du}{\sqrt{2(E + \Phi(u))}} \\ [\xi]_{\xi_{\text{lo}}}^{\xi} &= \int_{u_{\text{lo}}}^{u(\xi)} \frac{du}{\sqrt{2(E + \Phi(u))}} \end{aligned} \tag{38}$$

For $\Phi(u) = u^3$, as in the Ginzburg-Landau equation, the integral on the right of (38) is an elliptic integral, one of the standard special functions. However (38) is not immediately helpful in understanding the qualitative behavior of solutions to (36).

For more insight, we turn to the dynamical systems approach. Introducing

$$v \equiv \frac{du}{d\xi} \tag{39}$$

we can rewrite (36) as the dynamical system

$$\dot{u} = v \tag{40a}$$

$$\dot{v} = \frac{d\Phi}{du} - cv \tag{40b}$$

where $\dot{u}$, $\dot{v}$ are derivatives with respect to ξ. If $c = 0$, then the system (40) is **Hamiltonian**, i.e. there exists a Hamiltonian $\mathcal{H}(u, v)$ such that

$$\dot{u} = \frac{d\mathcal{H}}{dv} \tag{41a}$$

$$\dot{v} = -\frac{d\mathcal{H}}{du} \tag{41b}$$

which here is

$$\mathcal{H} = -\Phi + \frac{1}{2}v^2 \tag{42}$$

Let us analyze the reaction-diffusion system that results from adding diffusion to the normal form for a supercritical pitchfork bifurcation, leading to the **Ginzburg-Landau** equation:

$$\frac{\partial u}{\partial t} = \mu u - u^3 + \frac{\partial^2 u}{\partial x^2} \tag{43}$$

We integrate to obtain the potential

$$-\frac{d\Phi}{du} = \mu u - u^3 \qquad \Longrightarrow \qquad -\Phi = \frac{\mu}{2}u^2 - \frac{1}{4}u^4 \tag{44}$$

Steady states obey

$$0 = -\frac{d\Phi}{du} + \frac{d^2u}{dx^2} \tag{45}$$

Performing the transformation from space into time and separating (45) into two equations yields

$$\dot{u} = v \tag{46a}$$

$$\dot{v} = \frac{d\Phi}{du} \tag{46b}$$

As usual, we begin our analysis of (46) by finding its fixed points:

$$v = 0 \tag{47a}$$

$$\frac{d\Phi}{du} = 0 \quad \Longrightarrow \quad \bar{u}^3 - \mu\bar{u} = 0 \quad \Longrightarrow \quad \bar{u} = 0 \quad \text{or} \quad \bar{u} = \pm\sqrt{\mu} \tag{47b}$$

These values of $\bar{u}$ are the fixed points for the usual normal form without diffusion. The stability of $(\bar{u}, \bar{v})$ under the dynamics (46) is, however, quite different from that under the dynamics of the original system (43). The Jacobian of (46)

$$\begin{pmatrix} 0 & 1 \\ \Phi'' & 0 \end{pmatrix} = \begin{pmatrix} 0 & 1 \\ 3\bar{u}^2 - \mu & 0 \end{pmatrix} = \begin{pmatrix} 0 & 1 \\ -\mu & 0 \end{pmatrix} \quad \text{or} \quad \begin{pmatrix} 0 & 1 \\ 2\mu & 0 \end{pmatrix} \tag{48}$$

(where $\Phi'' \equiv d^2\Phi/du^2$) has eigenvalues

$$\lambda = \pm\sqrt{\Phi''} = \begin{cases} \pm\sqrt{-\mu} & \text{for} \quad \bar{u} = 0 \\ \pm\sqrt{2\mu} & \text{for} \quad \bar{u} = \pm\sqrt{\mu} \end{cases} \tag{49}$$

Note that the eigenvalues come in $\pm$ pairs, either imaginary or real (the trace of (48) is zero). This is typical for Hamiltonian systems, but rare for dissipative systems. Fixed points whose eigenvalues are imaginary pairs, i.e. centers, are called **elliptic**, while those whose eigenvalues are real pairs, i.e. saddles, are called **hyperbolic**.

Figure 7 illustrates the behavior of the Ginzburg-Landau equation for the two values $\mu = -1$ and $\mu = +1$. The top row illustrates the mechanical analogy. The potential $-\Phi(u)$ is shown as a function of u, along with the hyperbolic fixed points: $\bar{u} = 0$ for $\mu = -1$ and $\bar{u} = \pm\sqrt{\mu}$ for $\mu = +1$. Trajectories emanating from these fixed points are displayed. For $\mu = -1$, the trajectory leaving $\bar{u} = 0$ is unbounded and goes to $-\infty$. For $\mu = +1$, the trajectory leaving $\bar{u} = -\sqrt{\mu}$ at zero velocity arrives exactly at $\bar{u} = \sqrt{\mu}$ with zero velocity, since there is no friction. Figure 8 illustrates two more types of trajectories that may exist in the $\mu = +1$ case. On the left is a periodic oscillation: if u and $\dot{u}$ are sufficiently small, then the trajectory oscillates within the potential well, forever since there is no dissipation. On the right is an unbounded trajectory: if the initial position u and the initial velocity $\dot{u}$ are sufficiently large, then the trajectory can cross the potential well. Another type of unbounded trajectory also exists, in which the trajectory remains either to the left or to the right of the well.

The middle row of figure 7 illustrates this behavior from the dynamical systems point of view, by showing phase portraits of the two-dimensional dynamical system for $(u, \dot{u})$. For $\mu = -1$, the fixed point $(\bar{u}, \dot{\bar{u}}) = (0, 0)$ is a hyperbolic fixed point: the trajectories surrounding it are hyperbolas. The trajectory shown above it leaves $u = 0$ with a small positive velocity $\dot{u} = 0.1$ (otherwise it would not go anywhere) and goes to positive infinite $(u, \dot{u})$. For $\mu = +1$, the fixed point $(0, 0)$ is elliptic. Trajectories in the $(u, \dot{u})$ phase plane are elliptical. In the picture above, the particle would oscillate back and forth in the potential

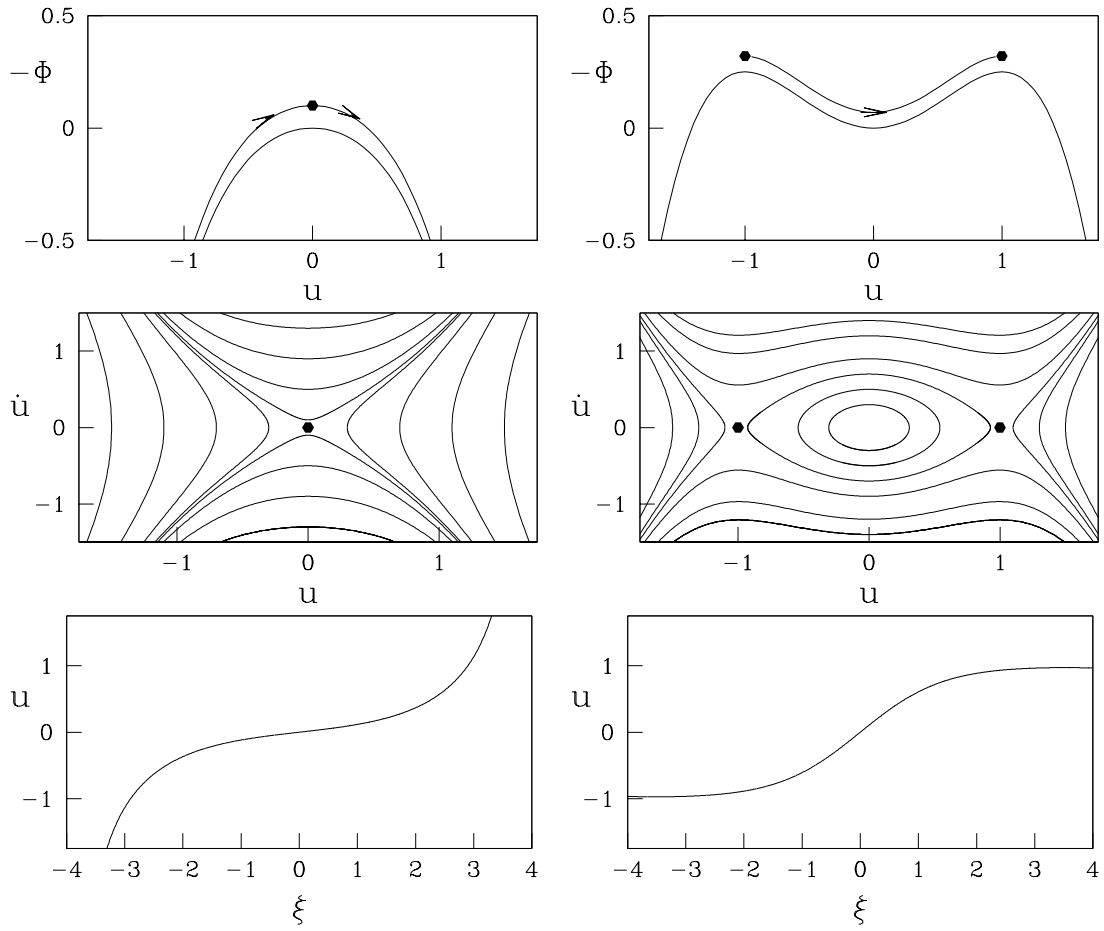

Figure 7: Behavior of the Ginzburg-Landau equation for $\mu = -1$ and for $\mu = +1$.
Top row: potential $-\Phi(u)$ with fixed points $\bar{u} = 0$ for $\mu = -1$ and $\bar{u} = \pm\sqrt{\mu} = \pm 1$ for $\mu = +1$. For $\mu = -1$, a portion of a trajectory is shown which originates at $u = -\infty$ and goes to $u = +\infty$. For $\mu = +1$, the trajectory shown goes from $\bar{u} = -1$ to $\bar{u} = +1$.
Middle row: phase portraits in the $(u, \dot{u})$ plane. $(0, 0)$ is a hyperbolic fixed point for $\mu = -1$ and an elliptic fixed point for $\mu = +1$. $(\sqrt{\mu}, 0)$ are hyperbolic fixed points for $\mu = +1$ and are connected by a heteroclinic orbit.
Bottom row: for $\mu = -1$, profile through $u = 0$ goes from $u = -\infty$ to $u = +\infty$. Profile through $u = 0$ is a front joining $\bar{u} = -1$ and $\bar{u} = +1$.

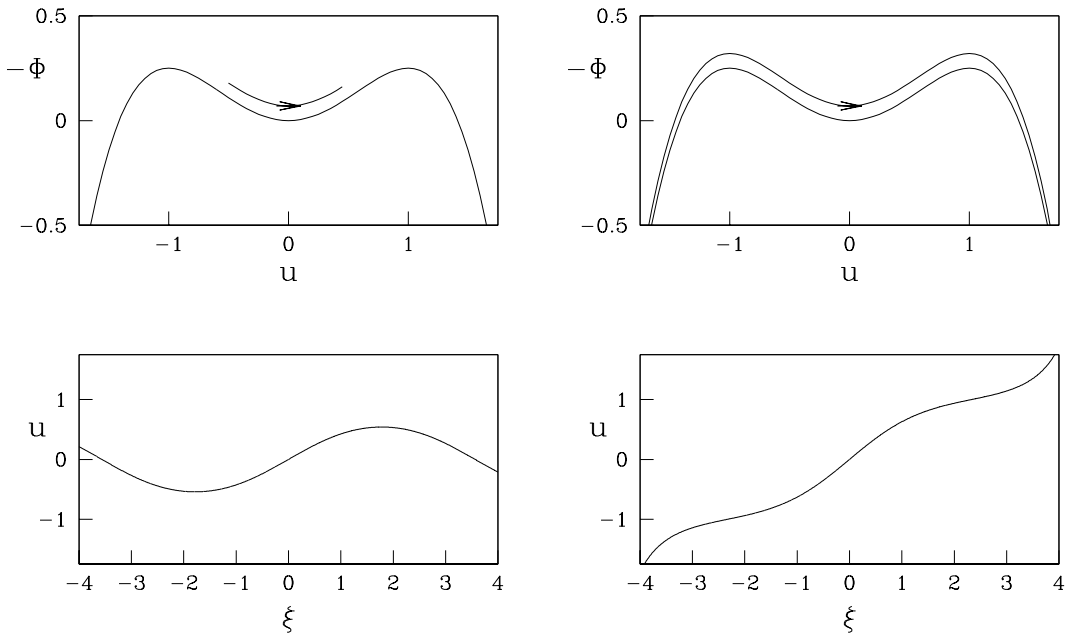

Figure 8: Behavior of the Ginzburg-Landau equation for $\mu = +1$ (continued).
First row: trajectory on left oscillates periodically in the potential well. Trajectory on right is unbounded.
Bottom row: Profile on left is a periodic wave. Profile on right is unbounded.

well. The elliptical trajectories are bounded by a limiting **heteroclinic orbit** joining the two hyperbolic fixed points $(\bar{u}, \dot{\bar{u}}) = (\sqrt{\mu}, 0)$ and illustrated in the row above it. There are also unbounded trajectories for $|u| > \sqrt{\mu}$ (to the left or right of the potential hills) or for $\dot{u}$ sufficiently large (the velocity is large enough for the trajectory to escape the potential well).

The bottom row illustrates the spatial analysis point of view, by considering the trajectories as u-profiles. For $\mu = -1$, the profile has $u = -\infty$ on the left, has an extended phase in the vicinity of $u = 0$ and then goes to $+\infty$ on the right. For $\mu = +1$, the profile has $\bar{u} = -1 = -\sqrt{\mu}$ on the left and, after a relatively narrow transition, attains the asymptotic value $u = 1 = \sqrt{\mu}$. That is, from the point of view of the original reaction-diffusion equation, the trajectory (heteroclinic orbit) at $\mu = +1$ is a **front** connecting the stable steady states $\bar{u} = \pm\sqrt{\mu}$ of the spatially homogeneous reaction equation. Figure 8 shows two more profiles, one periodic and one unbounded, which can also exist for $\mu = +1$.

Figures 7 and 8 show many possible trajectories (from the temporal point of view) or profiles (from the spatial point of view). Which one occurs is determined by the initial conditions (from the temporal point of view) or the boundary conditions (from the spatial point of view). For example, for $\mu = +1$, the boundary conditions $u(\pm\infty) = \pm 1$ lead to the profile on the right of figure 7. Periodic boundary conditions on a domain of fixed wavelength select the periodic profile on the left of figure 8.

Note that the front solutions connect two maxima of $-\Phi$, i.e. hyperbolic – and hence unstable – fixed points of (47). The reason for this is that these correspond to the *stable* spatially homogeneous solutions to the original system (32), as we now demonstrate. Spatially homogeneous solutions $\bar{u}$ to (32), i.e. solutions to

$$\frac{du}{dt} = -\frac{d\Phi}{du} \tag{50}$$

are extrema of Φ, satisfying $d\Phi/du = 0$. Their stability is determined by

$$-\frac{d^2\Phi}{du^2}(\bar{u}) \left\{ \begin{array}{c} < 0 \\ > 0 \end{array} \right\} \qquad \Longrightarrow \qquad \bar{u} \left\{ \begin{array}{c} \text{stable} \\ \text{unstable} \end{array} \right\} \tag{51}$$

Thus, homogeneous stable steady states are maxima of $-\Phi$, with $-d^2\Phi/du^2 < 0$.

So far, we have only considered the stationary case $c = 0$. We now focus on the effect of $c \neq 0$. We consider a front between $u_{-\infty}$ and $u_{+\infty}$, which are stable solutions to the spatially homogeneous equations. To do so, we impose boundary conditions

$$u(\xi = \pm\infty) = u_{\pm\infty} \tag{52}$$

with $u_{\pm\infty}$ the values at which $-\Phi$ attains its maximum values, which we denote by $\Phi_{\pm\infty} \equiv \Phi(u_{\pm\infty})$. Dirichlet conditions (52) at infinity necessarily imply homogeneous Neumann conditions:

$$\frac{du}{d\xi}(\xi = \pm\infty) = 0 \tag{53}$$

Travelling wave solutions obey

$$0 = c\frac{du}{d\xi} - \frac{d\Phi}{du} + \frac{d^2u}{d\xi^2} \tag{54}$$

We multiply (54) by $du/d\xi$ to obtain

$$0 = c\left(\frac{du}{d\xi}\right)^2 - \frac{d\Phi(u(\xi))}{d\xi} + \frac{1}{2}\frac{d}{d\xi}\left(\frac{du}{d\xi}\right)^2 \tag{55}$$

We integrate over the entire ξ interval, leading to:

$$\begin{aligned} 0 &= c\int_{-\infty}^{+\infty} d\xi \left(\frac{du}{d\xi}\right)^2 - \int_{-\infty}^{+\infty} d\xi \frac{d\Phi(u(\xi))}{d\xi} + \int_{-\infty}^{+\infty} d\xi \frac{1}{2}\frac{d}{d\xi}\left(\frac{du}{d\xi}\right)^2 \\ &= c\int_{-\infty}^{+\infty} d\xi \left(\frac{du}{d\xi}\right)^2 - [\Phi]_{-\infty}^{+\infty} + \frac{1}{2}\left[\left(\frac{du}{d\xi}\right)^2\right]_{-\infty}^{+\infty} \end{aligned} \tag{56}$$

The last term in (56) vanishes due to (53), and we obtain

$$c = \frac{\Phi_{+\infty} - \Phi_{-\infty}}{\int_{-\infty}^{+\infty} d\xi \left(\frac{du}{d\xi}\right)^2} \tag{57}$$

Equation (57) shows that the front velocity is positive if $\Phi_{-\infty} < \Phi_{+\infty}$, i.e. if $-\Phi_{-\infty} > -\Phi_{+\infty}$. If the front velocity is positive, then the front moves from left to right and the domain over which $u = u_{-\infty}$ increases while the domain over which $u = u_{+\infty}$ shrinks. Thus the front moves so as to increase the size of the domain with greater $-\Phi$. In terms of the mechanical analogy, the trajectory goes from $u_{-\infty}$, with potential $-\Phi_{-\infty}$, to $u_{+\infty}$, with lower potential $-\Phi_{+\infty}$. In order for the "velocity" $du/d\xi$, and thus the kinetic energy, to vanish at both endpoints, energy must be lost via friction. Hence c is positive.

In this context, "negative friction" is possible since c negative merely means that the front moves towards the left. According to (57), this happens when $-\Phi_{+\infty} > -\Phi_{-\infty}$, i.e. when the trajectory goes to a location with higher potential energy.

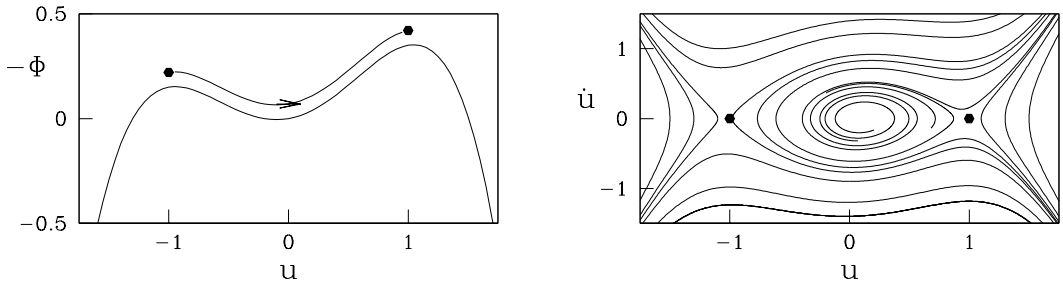

Figure 9: Behavior of perturbed Ginzburg-Landau equation. A trajectory leaving the hill on the left arrives at the higher hill on the right, using "negative friction" to increase its energy. In the phase portait, it can be seen that the former center has become a focus, surrounded by spiralling trajectories.

Figure 9 illustrates the behavior of the perturbed Ginzburg-Landau equation

$$0 = c\frac{du}{d\xi} + \mu u - u^3 - 0.1 + \frac{d^2u}{d\xi^2} \tag{58}$$

whose potential

$$-\Phi = \frac{1}{2}\mu u^2 - \frac{1}{4}u^4 - 0.1u \tag{59}$$

has two maxima of different heights. The trajectory goes from the lower hill to the higher hill, increasing its "energy" via "negative friction".

5 Exercises

1. Consider the solution of equation

$$0 = -\frac{d\Phi}{du} + \frac{d^2u}{dx^2} \tag{60}$$

for the function $\Phi(u)$ shown on figure 10.

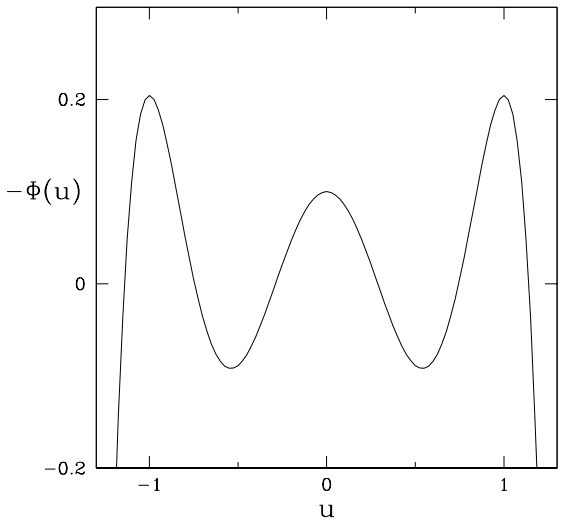

Figure 10: Potential $-\Phi(u)$.

a. Write (60) as a two-variable dynamical system in $(u, v = du/dx)$. Show that this dynamical system is Hamiltonian.

b. State the location and the nature of the fixed points of the dynamical system in **a.**

c. Construct a phase-plane portrait in the (u, v) parameter plane. Include all heteroclinic and homoclinic orbits.

d. Draw the qualitative form of possible profiles $u(x)$ corresponding to the trajectories in the (u, v) phase plane. Indicate these profiles on graphs of $-\Phi(u)$.

2. Show that the system

$$\dot{x} = \sin y \tag{61a}$$

$$\dot{y} = x \cos y \tag{61b}$$

is a potential system (and thus has no limit cycles).